

Hydrogen-Bonding Interactions in Cinchonidine–2-Methyl-2-Hexenoic Acid Complexes: A Combined Spectroscopic and Theoretical Study

Daniel M. Meier, Atsushi Urakawa, Natascia Turrà, Heinz Rügger, and Alfons Baiker*

Institute for Chemical and Bioengineering, Department of Chemistry and Applied Biosciences, ETH Zurich, Hönggerberg, HCI, 8093 Zurich, Switzerland

Received: March 03, 2008; Revised Manuscript Received: April 16, 2008

Molecular interactions between cinchonidine (CD) and 2-methyl-2-hexenoic acid (MHA) have been studied by means of NMR, ATR-IR MES, DFT, and ab initio molecular dynamics. These interactions are of particular interest due to their pivotal role in the chiral induction occurring in the heterogeneous catalytic asymmetric hydrogenation of α,β -unsaturated acids. The population density of the Open(3) conformer of CD, the most populated one at room temperature in apolar solvents, considerably increased to a maximum by addition of MHA to CD in toluene. The CD–MHA complex showed prominent symmetric and asymmetric carboxylate stretching vibrations in the regions of 1350–1410 and 1520–1580 cm^{-1} , respectively. DFT calculations revealed that these vibrational frequencies are expected to significantly shift depending on the chemical surrounding of MHA, that is, the hydrogen bond network. Earlier postulated 1:1 binding between CD and MHA was considered unlikely; instead, a dynamic equilibrium involving the MHA monomer and dimer, the 1:3 and possibly 1:2 CD–MHA complexes, were rationalized. Stable CD–MHA structures suggested by DFT calculations are the “1:3, halfN, cyclic” and the “1:3, halfN, cyclic tilted” complexes, where three MHA molecules are connected in wire by hydrogen bonding, two having direct interaction with CD. The confinement of CD’s torsional motions in the complexes, leading to a slightly distorted Open(3) conformer via specific hydrogen-bonding interactions, was clearly reproduced by ab initio molecular dynamics, and the stable and flexible nature of the interaction was verified. Theoretical IR spectra of the complexes reproduced the characteristic vibrational frequencies of the complexes observed experimentally, supporting the stability of the 1:3 and implying the possibility of even higher molecular weight CD–MHA complexes.

Introduction

Intermolecular hydrogen bonding, which is largely responsible for the generation of supramolecular complexes, is an eminent and still expanding research field. The noncovalent structures of flexible nature play key roles in a broad chemical range, including chiral recognition and catalysis.¹ The interactions are well-known in liquid-phase chemistry, for example, homogeneous catalysis where they promote regioselective reactions² or induce stereoselectivity.³ Such interactions are also understood to occur in heterogeneous catalysis, as, for example, in the asymmetric hydrogenation of activated ketones⁴ or, as studied here, of α,β -unsaturated carboxylic acids. Thereby, metal surfaces are modified by adsorbing a chiral molecule, the so-called chiral modifier or simply modifier. In general, Pd chirally modified by cinchona alkaloids, employed in the enantioselective hydrogenation of the carboxylic acid’s substituted C=C double bond, are proven to be efficient for this reaction.⁵ An overview of the reaction and a variety of prochiral acids hydrogenated in this way are summarized in different reviews.^{6–12} In contrast to the continuous improvement of the enantiomeric excess (ee) up to 92%¹³ by systematically varying the reaction conditions,¹⁴ substrates,¹⁵ and additives,¹⁶ the mechanistic understanding of the reaction lags somewhat behind and is a matter of debate in the literature. This is certainly in part due to the inherent complexity of the reaction involving a substrate, modifier, solvent, and catalyst surface. Better insight into the reaction

mechanism, especially the interaction between the modifier and substrate, is crucial towards the rational design of the catalytic system.

The focus of the current study is on the interaction between the chiral modifier, cinchonidine (CD), and 2-methyl-2-hexenoic acid (MHA) in solution, in view of the commercial importance of chiral carboxylic acids^{17,18} and the good ee afforded for this reaction using CD and MHA.^{19,20} A combined spectroscopic and theoretical approach was deemed suitable to study the CD–MHA interaction and gain deeper insight into the reaction mechanism. In solution phase, two very powerful spectroscopic techniques are IR and NMR, being largely complementary due to their significantly different sensitivity relative to structural changes and bonding information. An absolute necessity, considering the complexity of the system, was theoretical support, in particular, for the IR signal assignment and the structural characterization.

From earlier spectroscopic^{21–27} and theoretical^{28,29} studies, it is known that CD and other cinchona alkaloids exist preferably in the Open(3) conformation, especially in apolar solvents.²² Upon addition of an acidic substrate to CD or employing an acidic solvent, the population of the Open(3) conformer is further enhanced.^{30–32} Similarly, simple protonation of the quinuclidine N of CD and the presence of a counterion can drastically influence the conformational behavior and leads also to an increase in Open(3).³¹ In the case of the CD–acid interaction, the origin of the enhancement of the Open(3) population has been assigned to the confinement of two characteristic torsion angles of CD (τ_1 and τ_2 , Figure 1) via a

* To whom correspondence should be addressed. E-mail: baiker@chem.ethz.ch.

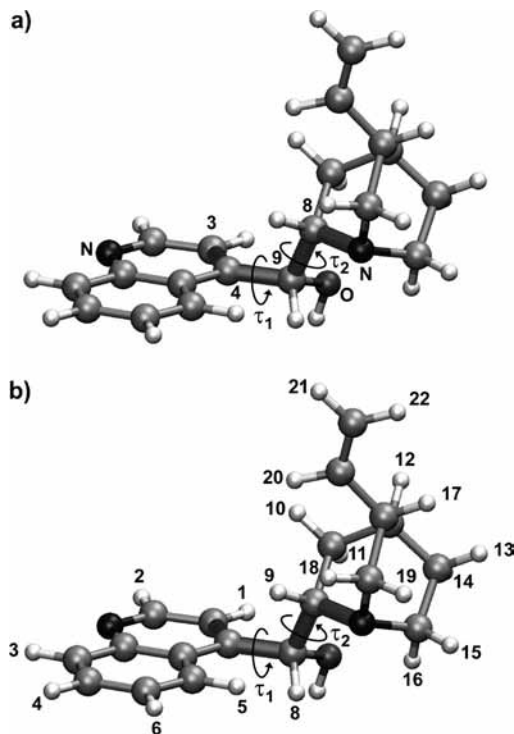


Figure 1. Open(3) conformer of CD. The two characteristic torsion angles τ_1 and τ_2 are indicated. Definitions of carbon and proton numbering are shown in a) and b), respectively.

specific interaction between the quinuclidine N of the modifier and the carboxylic acid.^{30,33} It was suggested that one or two acid molecules bind to CD, forming 1:1 and 1:2 modifier–acid complexes. Two possible structures for the 1:1 complex have been proposed, a monodentate interaction³⁴ where the acidic proton interacts with the basic N of the quinuclidine and a bidentate interaction^{35,36} where an additional hydrogen bond between the hydroxyl H of the CD and the carbonyl O of the acid is formed. Extended and more flexible hydrogen bond networks involving two acid molecules in 1:2 complexes have been suggested as well.^{30,33,37,38}

Furthermore, a solvent-polarity-dependent modifier to acid ratio was postulated to explain the change in ee on differently dispersed catalysts.³⁹ Previous FT-IR studies using acetic and tiglic acid show that more than one acid molecule interacts with the modifier, already at a CD:acid ratio of about 2:1.^{30,33} Plausible 1:1 and 1:2 structures were theoretically studied for the CD–acetic acid system.³⁰

In this work, we have extended the CD–acid interaction model by taking three acid molecules into account in the hydrogen bond network. Conformational aspects and the interaction network between CD and MHA were investigated by NMR and IR, respectively, and critically compared with theoretical investigations.

Experimental Section

Chemicals. Chemicals were used as received. Toluene ($\geq 99.7\%$) and CD ($\geq 98\%$) were purchased from Fluka and MHA ($\geq 98\%$) was purchased from ABCR. MHA was determined to be present as an (*E*)-isomer based on ¹H-NMR, ¹³C-NMR, HH-NOESY proton spectra, and comparison with NMR prediction as well as with (*E*)-2-methyl-2-pentenoic acid studied in the literature.⁴⁰ Toluene-*d*₈ ($\geq 99.8\%$, Dr. Glaser AG Basel) was used for the NMR experiments. Solutions were saturated

with hydrogen (PanGas, 5.0) and nitrogen (PanGas, 5.0) in the ATR-IR experiments.

NMR. NMR spectra were recorded using Bruker Avance AV-500 and AV-700 MHz spectrometers. Signal assignments were assisted by correlation spectroscopy (COSY), total correlation spectroscopy (TOCSY), and low-temperature experiments (193–300 K). Conformational information was obtained by nuclear Overhauser enhancement spectroscopy (NOESY) and vicinal coupling constants. The standard solutions measured contained 2.5 mM CD or 2.5 mM CD and 5 mM MHA in toluene-*d*₈. Low concentration was required to suppress auto-aggregation⁴¹ and precipitation⁴² and also to have a better comparison with theoretical results where no solvent and no intermolecular interactions are considered. For the NOESY experiment, the free precession time ($t_{1\max}$), the mixing time (τ_m), the acquisition (AQ), and the relaxation time were 80 ms, 0.7 s, 0.205 s, and 2 s, respectively. In the TOCSY experiment $t_{1\max}$, the spin lock time, AQ, and the relaxation time were 70 ms, 80 ms, 0.307 s, and 0.8 s, respectively.

Transmission FT-IR. A commercial IR cell (Portmann Instruments) equipped with rectangular CaF₂ windows was used for recording IR transmission spectra at room temperature. The path length was set at 25 μm by means of a Teflon spacer. IR spectra were collected with a Bruker Equinox 55 at 4 cm^{-1} resolution with a liquid-nitrogen-cooled MCT detector. A spectrum of pure toluene served as the reference.

ATR-IR MES. Infrared spectra were measured on a Bruker IFS 66/S FT-IR spectrometer equipped with an ATR-IR attachment (Optispec) and a liquid-nitrogen-cooled MCT detector. All spectra were recorded at 4 cm^{-1} resolution. The IRE (internal reflection element, Ge, 50 \times 20 \times 2 mm) was fixed within a stainless steel flow-through cell specially designed for fast switching between two flow lines. A more detailed description of the cell is reported elsewhere.⁴³ The temperature of the flow-through cell was regulated by means of a thermostat (Julabo F25) at 298 K. The solution flow (0.54 mL/min) was controlled by means of a peristaltic pump (ISMATEC Reglo 100) located behind the cell. The entrance of two flow lines was altered by two computer-controlled pneumatically actuated three-way Teflon valves (Parker PV-1-2324).

Modulation excitation spectroscopy (MES) was combined with ATR-IR spectroscopy, typically used in the investigation of solid–liquid interfaces.⁴⁴ Here, the MES technique was employed to simply analyze the solution phase. The great sensitivity enhancement allows detection of very small signals, as those in this study originating from modifier–carboxylic acid interactions, by alternately flowing two solutions periodically, for example, first a solvent (e.g. CD in toluene) and second a solution (e.g. CD and MHA in toluene). MES removes all of the signals in common in the two flows, reduces noise, and further enhances the difference signals between the two flows (e.g. interaction signals due to CD–MHA) by means of phase-sensitive detection.^{45,46} The CD–MHA interaction signals were on the order of 10–100 microabsorbances, which would otherwise be very difficult to achieve for confident identification. Only in-phase spectra⁴⁶ are shown in this work.

The experimental series started with the modulation experiment, that is, alternating flow of MHA in a 2.5 mM CD solution versus a 2.5 mM CD solution. Different concentrations of MHA were used for the modulation experiments: 0.5, 1.25, 2.5, and 5.0 mM, which correspond to 0.2, 0.5, 1.0, and 2.0 acid equivalents, respectively. For comparison, the MES experiment of MHA in toluene versus toluene was performed. Four dummy

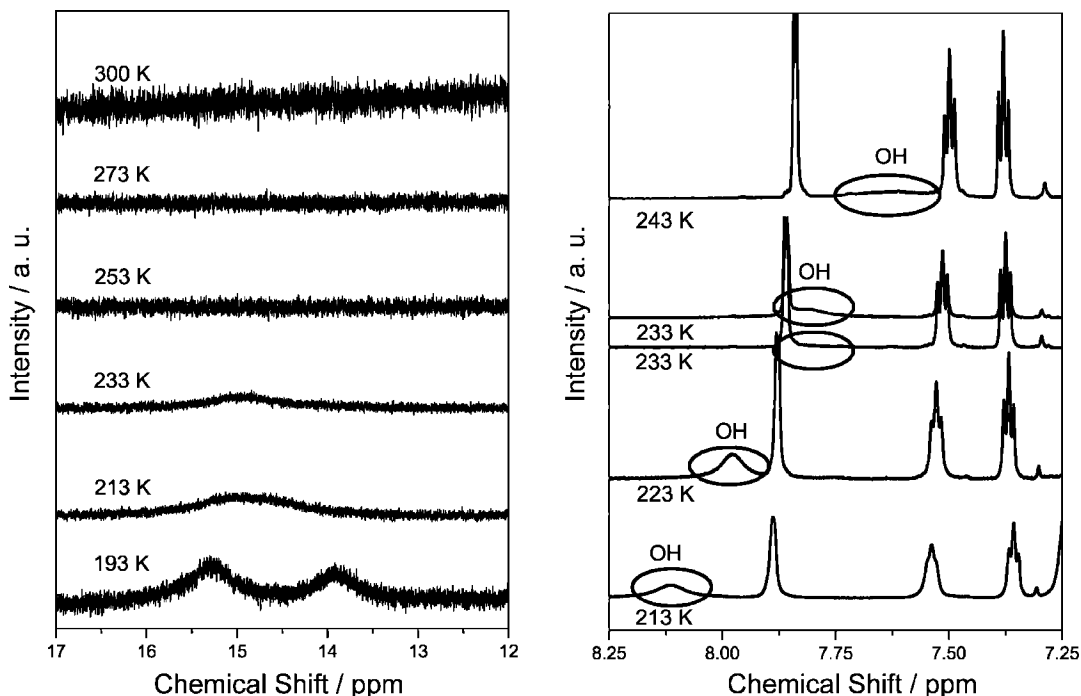


Figure 2. ^1H -NMR spectra of the acidic (left) and hydroxyl (right) protons in 2.5 mM CD and 5 mM MHA solution in toluene- d_8 at different temperatures.

and 10 measurement cycles with 60 data points per cycle were measured in the MES experiments.

Computational Methods. Geometry optimization, single-point energy, vibrational frequency calculations within harmonic approximation, and ab initio molecular dynamics were performed with the B3PW91 hybrid functional^{47,48} using Gaussian 03⁴⁹ and with the BLYP functional^{48,50} using Car–Parrinello molecular dynamics (CPMD).⁵¹ The first and the second methods are noted hereafter as B3PW91-G and BLYP-PW, respectively. A 6-311G(d,p) basis set was applied for all of the atoms for the B3PW91-G method. Basis set superposition error (BSSE) due to the Gaussian basis sets was corrected by the counterpoise approximation⁵² for selected complexes with a bimolecular interaction. Zero-point energies were corrected. The BLYP-PW applied plane wave basis sets (energy cutoff: 70 Ry) within a cubic cell of 24 Å length. Norm-conserving Troullier–Martins pseudopotentials were used to describe the interaction between the valence electrons and the ionic cores.⁵³ All calculations were performed as an isolated gas-phase molecule or complex without solvent effects. IR spectra are shown as the sum of Lorentzian lines taking the calculated IR intensity of a normal mode as the height at each frequency. The calculated vibrational frequencies were scaled by 0.96. For ab initio molecular dynamics simulations, the BLYP-PW method was used with an electronic fictitious mass of 600 au and a time step of 5 au (0.121 fs).

Results and Discussion

NMR Investigation. The conformation of CD is best described by two dihedral angles defining the relative spatial positions of the modifier's quinuclidine and quinoline moiety, τ_1 ($\text{C}_3\text{--C}_4\text{--C}_9\text{--C}_8$) and τ_2 ($\text{C}_4\text{--C}_9\text{--C}_8\text{--N}$), as indicated in Figure 1. CD is shown in its Open(3) conformation, where the quinuclidine nitrogen atom points away from the aromatic quinoline moiety. Structures of other stable conformers can be found elsewhere.^{22,28,54,55} In order to determine the CD conformation, the coupling constant between H_8 (δ 5.3) and H_9 (δ 3.1), $^3J_{\text{H}_8\text{--H}_9}$, was studied. This coupling constant is sensitive

to changes in (i) the angle of τ_3 ($\text{H}_9\text{--C}_8\text{--C}_9\text{--H}_8$) and (ii) the population density of Open or Closed CD conformations.^{22,30}

Interestingly, upon addition of 2 equiv of MHA to the CD solution, the H_8 signal shifted from δ 5.13 to 6.19, while $^3J_{\text{H}_8\text{--H}_9}$ decreased from 4.3 to 1.6 Hz. The decrease in $^3J_{\text{H}_8\text{--H}_9}$ indicates higher populations of conformers with τ_3 close to $\pm 90^\circ$, implying the conformation changes to be more Open in the presence of the acid. Also, 2D NOESY experiments on the CD–MHA mixture were performed to gain additional structural information (the spectra are shown in the Supporting Information), and the data were analyzed by NOESY-DFT analysis reported elsewhere.⁵⁵ Strong NOEs between $\text{H}_5\text{--H}_8$ and $\text{H}_5\text{--H}_9$, indicative of the Open(3) conformer, were observed. Additional clear evidences for the Open(3) conformer were given by the NOEs between H_1 and H_{11} and a weak signal of H_8 with H_{16} . $^3J_{\text{H}_8\text{--H}_9}$ and NOESY-DFT analyses revealed that the Open(3) conformer was largely predominant in the presence of 2 equiv of MHA. Furthermore, addition of MHA shifted a number of ^1H signals significantly with respect to the pure CD (the spectrum is shown in the Supporting Information). Around δ 3.4, a prominent broad signal, assigned to the alcoholic, acidic, and aqueous protons, arose. The broadness indicates a highly dynamic nature of interactions and the exchange between them. By stepwise cooling of the solution from 300 to 193 K in 20 K steps, the broad signal split, and individual protons could be distinguished. Figure 2 (left) shows that below 233 K, a signal at around δ 14.8 appeared. At 193 K, two distinct signals were detected at δ 13.9 and δ 15.3, assigned to the proton bound to quinuclidine N of CD and the acidic proton, respectively. In the right panel of Figure 2, the gradual shift of the CD-hydroxyl proton from δ 3.4 at 300 K to δ 8.1 at 213 K is evident. Two spectra measured at 233 K are shown. The lower one illustrates that the alcoholic proton signal of CD disappears by presaturation at δ 14.8, proving that chemical exchange occurs between the acidic and alcoholic proton. Signals due to water, contained in the purchased CD, were not detected below 248 K.

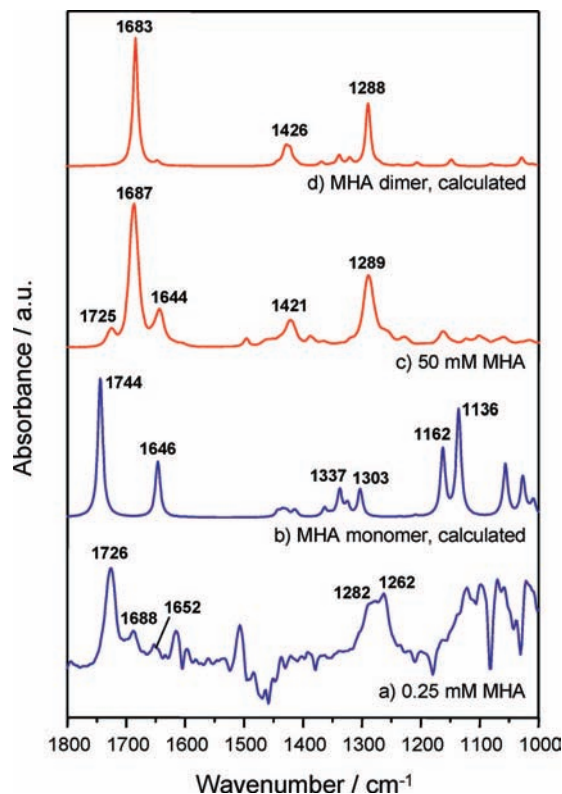


Figure 3. Experimental IR spectra of 0.25 (a) and 50 mM (c) MHA in toluene and theoretical IR spectra of MHA monomer (b) and dimer (d), calculated by the B3PW91-G method. The frequencies are scaled by 0.96.

Unambiguously, the NMR experiments showed that upon addition of the acid to CD, the population equilibrium between the different conformers shifted almost completely towards the Open(3) conformer. This is in good agreement with the conformational change reported for the protonation of CD.^{31,32} The important finding of the current study is the discrimination of two different acidic protons at low temperature and the observation of exchange processes occurring between the CD hydroxyl proton and the acidic protons, which persist even at low temperature. This is consistent with a picture of molecular interaction of MHA with both the basic nitrogen and the hydroxyl group of the CD. A twofold modifier–acid interaction seems crucial for asymmetric induction. Employing a derivatized modifier, that is, by substituting the CD hydroxyl group with an organic rest, led to racemic product mixtures in the hydrogenation of α,β -unsaturated acids.⁵⁶ From the NMR experiments, however, it was not possible to establish whether the modifier–carboxylic acid interaction results in a 1:1, 1:2, 1:3, or higher ratio complex, or even in a combination of these, nor could the exact form of the intermolecular interaction be resolved. Therefore, we studied the nature of the dynamic interactions by IR, which allows investigation at a much shorter time scale.

IR Investigation. Prior to the IR study on the CD–MHA interaction, IR bands originating from MHA monomers and dimers were investigated. Spectra were measured for diluted (0.25 mM) and concentrated (50 mM) toluene solutions of MHA in order to assign bands due to isolated and dimeric forms of MHA, respectively. Both spectra were recorded in the transmission mode and are shown in Figure 3 in comparison to the theoretical spectra of monomeric and dimeric MHA calculated by the B3PW91-G method. On the basis of this comparison, MHA exists mainly as a dimer (Figure 3c and d, for example,

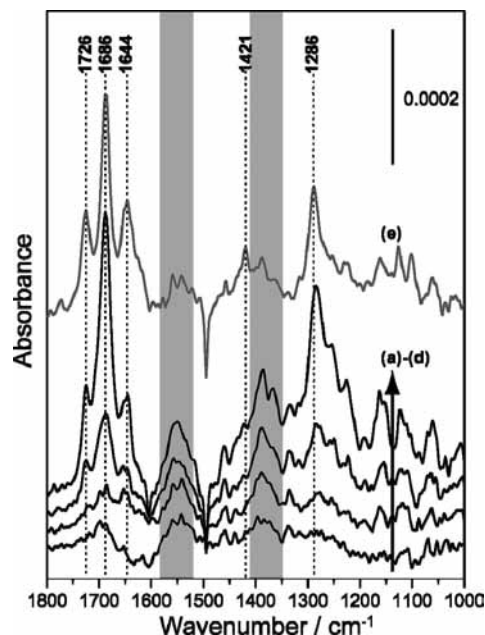


Figure 4. IR spectra obtained by ATR-IR MES. The compositions of two flows used in the MES experiments are MHA,CD:CD = (a) 0.5,2.5; 2.5 mM, (b) 1.25,2.5;2.5 mM, (c) 2.5,2.5;2.5 mM, (d) 5.0,2.5;2.5 mM, and (e) 2.5,0:0 mM.

bands at approximately 1290 and 1425 cm^{-1} due to $\delta(\text{O-H})$ and $\delta(\text{C-H})$ and 1685 cm^{-1} due to $\nu_{\text{as}}(\text{C=O})$ in the 50 mM solution, while bands of the monomer could also be assigned at 1644 ($\nu(\text{C=C})$) and 1725 cm^{-1} ($\nu(\text{C=O})$) based on the theoretical IR spectrum of the monomer (Figure 3b). The dimer considered in the calculation has the cyclic structure where the two units connect via hydrogen bonds. The excellent agreement between the experimental and theoretical spectra of the MHA dimer assures the reliability of the method used for IR spectra calculations, which also implies a high accuracy of the calculated molecular or complex structure, in particular, connected by hydrogen bonds as CD–MHA complexes. For the diluted, 0.25 mM MHA solution (Figure 3a), MHA exists dominantly as a monomer, as evidenced by the intense band at 1726 cm^{-1} . The dimer seems also to be present at the 0.25 mM concentration, as seen from the small absorption at 1688 cm^{-1} . The poor quality of the latter spectrum (Figure 3a) and the unsatisfying agreement with the theoretical spectrum of the monomer (Figure 3b) are due to the low concentration and probably an interaction with the solvent molecules which could not be taken into account by our calculations.

Next, the CD–MHA interactions were investigated by ATR-IR MES (Figure 4a–d). The CD concentration was set constant at 2.5 mM, and the MHA concentration was stepwise increased from 0.2 to 2.0 equiv with respect to CD. In the regions of 1350–1410 and 1520–1580 cm^{-1} (highlighted in the figure), broad and slightly growing signals appeared, with absorbance being on the order of 10^{-4} . Such a very high sensitivity and excellent suppression of solvent signals could be achieved as a result of the application of the MES technique.⁴⁶ The negative signals around 1500 cm^{-1} in Figure 4 are an experimental artifact due to the very small concentration difference of toluene used in the two flows (of CD and CD + MHA solutions). The observed broad signals belong neither to MHA (Figure 3) nor to CD;⁵⁷ they originate from the intermolecular interactions between the modifier and the acid. The interaction signals could be observed already at the lowest ratio of 0.2 (Figure 4a) and did not proportionally increase at higher MHA concentrations.

In addition, alteration of the CD–MHA ratio did not shift the band positions nor did it affect their broad shapes. In the same frequency region, signals due to the interaction of acids with CD had been observed previously by transmission IR.^{30,33,38} Generally, broad signals indicate a high flexibility of a system, dynamic processes, and various possible configurations near the energetic minima. This implies a highly flexible and dynamic nature of the CD–MHA interaction. The two regions where the interaction signals were observed are typically assigned to asymmetric ($1550\text{--}1610\text{ cm}^{-1}$) and symmetric ($1400\text{--}1450\text{ cm}^{-1}$) carboxylate vibrations.⁵⁸ Figure 4e shows the spectrum of MHA measured by ATR-IR MES (one flow with MHA in toluene and the other with toluene). The concentration of MHA is equal to that in the spectrum (c) of Figure 4 where the CD–MHA ratio is 1:1. At this 1:1 ratio, all signals due to the acid in its monomeric and dimeric forms could be detected; however, they were significantly reduced in intensity in the presence of CD. The signals of MHA were marginal up to the CD–MHA ratio of 1:0.5 (1.25 mM MHA) compared to the broad signals due to the CD–MHA complex. Under these conditions, the MHA concentration (1.25 mM) is five times higher than that in the diluted MHA solution shown before (Figure 3a); hence, the absence of the expected monomer and dimer signals clearly corroborates a stronger interaction between CD and MHA than that between MHA molecules. In contrast to the transmission IR studies with CD, acetic acid,³⁰ and tiglic acid,³³ no signal shifts or shoulders were detected in the spectral region of $1520\text{--}1580\text{ cm}^{-1}$, probably due to the use of different substrates and solvents. The lack of a band shift in the “interaction regions” of the CD–MHA complex implies a preferred arrangement, independent of the modifier–acid ratio.

Concluding, it can be stated that the IR experiments revealed a specific CD–MHA interaction, starting to appear at CD-to-MHA ratios slightly higher than 1:0.2. Despite the clear indication of this interaction influencing the carboxylate vibrations, as clearly evidenced from their near absence at the high CD-to-MHA ratios (Figure 4a and b), unfortunately, no conclusive structural information could be obtained from the IR spectra. In the next section, we would like to shed light on the nature of the CD–MHA interaction and preferred specific interaction networks based on the stabilities of various CD–MHA complexes as well as the structural investigations.

Theoretical Investigation. CD–MHA Complexes. CD–MHA interactions were studied in detail, considering various types of 1:1, 1:2, and 1:3 CD–MHA complexes. In all cases, we restricted the search to the Open(3) conformers of CD based on the NMR results discussed previously. Potential minima structures of CD–MHA complexes are illustrated in Figure 5. A stable 1:1 complex can be expected, having hydrogen bonds between the quinuclidine N and the hydroxyl group of the acid and between the hydroxyl group of CD and the carboxyl group of MHA. Possible monodentate 1:1 complexes containing either one or the other interaction were ruled out due to their inherent low stability³⁰ and due to the necessity of a twofold interaction for the induction of product chirality.^{35,56} For the 1:2 ratio, three different interaction modes were considered. The one called “1:2, cyclic” forms a cyclic hydrogen bond network where two MHA molecules are connected in chain, forming a third hydrogen bond between two MHA molecules. The two other complexes are, in principle, similar to the “1:1”, the difference being that in the complex “1:2, halfO”, the second MHA molecule forms a hydrogen bond to the O of the first acid where the hydroxyl group of CD is interacting, while in the “1:2, halfN” complex, the second acid

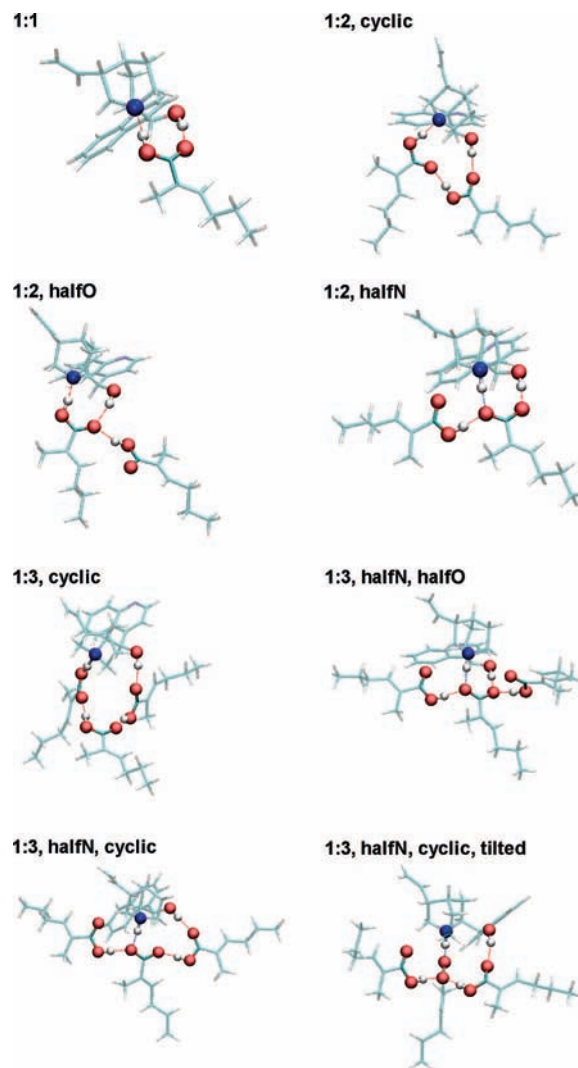


Figure 5. Investigated 1:1, 1:2, and 1:3 CD–MHA complexes.

molecule forms a hydrogen bond to the acid O where it interacts with the quinuclidine N of CD. The minimum-energy structures and the binding energies (B.E.) for these complexes were evaluated by two DFT methods, the B3PW91-G and the BLYP-PW methods, in order to compare the influence of different functionals and basis sets. The B.E.s calculated using the B3PW91-G method were consistently higher (Table 1). This is most likely because of the BSSE caused by the Gaussian basis sets. The correction of the BSSE for the first two bimolecular complexes yielded B.E. values close to those calculated using the second method, indicating that the B.E. differences are largely due to the BSSE. The acid dimer shows higher stability than that of the 1:1 complex. Our IR results, however, revealed a stronger CD–MHA interaction compared to the MHA intermolecular interactions, hence rendering the possible presence of the 1:1 interaction. The 1:2 complexes are significantly more stable with respect to the 1:1 complex. Among the 1:2 complexes, the “1:2, halfN” and the “1:2, cyclic” have about the same B.E.s. The “1:2, halfN” is similarly stable based on the BLYP-PW method but less stable based on the B3PW91-G method. The “1:2, halfO” shows a considerably smaller B.E. than those of the other 1:2 complexes.

Furthermore, four 1:3 complexes based on the stable “1:2, cyclic” or “1:2 halfN” were studied (Figure 5). All of these are combinations of the structural motifs discussed above. In (i) the “1:3, cyclic” CD interacts with three acid molecules, forming

TABLE 1: Binding Energies (B.E.) and N–H Bond Lengths from Quinuclidine N to the Closest Acid Proton Obtained by Two Different DFT Methods for the Respective CD–MHA Complexes^a

	B3PW91-G		BLYP-PW
	B.E./kcal mol ⁻¹	N–H bond length/Å	B.E./kcal mol ⁻¹
MHA–dimer	17.6	1.62	15.5
1:1	15.7	1.61	12.2
1:2, cyclic	27.0	1.52	21.5
1:2, halfO	22.2	1.57	16.9
1:2, halfN	25.7	1.08	21.6
1:3, cyclic	35.0	1.47	28.0
1:3, halfN, halfO	35.8	1.07	29.1
1:3, halfN, cyclic	37.0	1.07	30.4
1:3, halfN, cyclic tilted	36.5	1.08	30.2

^a BSSE-corrected B.E. MHA–dimer: 14.7 kcal mol⁻¹.

a hydrogen-bonding chain. (ii) “1:3, halfN, halfO” is a combination of the “1:2, halfN” and the “1:2, halfO” complex, whereas (iii) “1:3, halfN, cyclic” is the combination of the “1:2, halfN” and the “1:2, cyclic” complex. In (iv) “1:3, halfN, cyclic, tilted”, the central acid molecule is tilted by $\sim 90^\circ$ with respect to the “1:3, halfN, cyclic” complex, having the two acid protons interacting with the carboxyl oxygen of the acid. Table 1 clearly shows the high stability of the 1:2 and 1:3 complexes and also a nearly linear increase in B.E. proportional to the number of acid molecules in the complexes. Among the 1:3 complexes, the “1:3, halfN, cyclic” is the most stable one found by both DFT methods, followed by the “1:3, halfN, cyclic, tilted”. Furthermore, the acidity of MHA, leading to the protonation of quinuclidine N, seems to be greatly influenced by the characteristics of the hydrogen bond network. As a general trend, shorter H \cdots N distances are connected with higher binding energies (Table 1). This tendency infers a major electrostatic contribution to the CD and MHA interaction, effectively forming an ion pair, whose binding energy is greatly influenced by the coordination ratio (1:1, 1:2, or 1:3) and the relative spatial arrangement of CD and the acid. Similarly, much higher binding energies have been observed for protonated amines interacting with methyl pyruvate than those for neutral amines interacting with the same substrate.^{59,60}

Comparison between Experimental and Theoretical IR Spectra. Figure 6 compares the experimental IR spectra with the calculated ones obtained for the different complexes by the B3PW91-G method. The IR spectrum of the deprotonated MHA, the MHA anion, serves as a reference for the carbonyl stretches, $\nu(\text{COO})$, without intermolecular interaction. The frequency regions expected to contain the signals originating from the modifier–acid interactions are highlighted. The MHA anion has no bands in these highlighted regions; the experimentally detected signals in this region do not likely arise from free carboxylate vibrations. The shifts of the carboxylate stretching frequencies are probably due to the presence of a hydrogen bond network. This holds, for example, for the 1:1 complex, whose signals are calculated to be in the same region as those of the acid and the MHA anion. On the other hand, the bands arising from the 1:2 complexes are considerably different. What remarkably differentiates these three spectra of the 1:2 complexes are red and blue shifts of the $\nu_{\text{as}}(\text{COO})$ and the $\nu_{\text{s}}(\text{COO})$, respectively, steadily increasing from the “1:2, cyclic”, the “1:2, halfO”, to the “1:2, halfN”. In particular, the $\nu_{\text{as}}(\text{COO})$ of the “1:2, halfN” appears in the highlighted region. Normal mode analysis clarified that the bands in or close to the “interaction” regions are due to the MHA $\nu(\text{COO})$, which interacts with the quinuclidine N of CD. A number of bands in the nonhighlighted regions are due to other MHA $\nu(\text{COO})$, partially combined with the vibrations of the CD skeleton.

Calculations for the 1:3 complexes generally reproduced best the experimentally observed shifts of $\nu_{\text{s}}(\text{COO})$ and $\nu_{\text{as}}(\text{COO})$, and the bands are indeed located in the highlighted region (Figure 6). Similar to the 1:2 complexes, the vibrations in the “interaction” regions arise from the MHA $\nu(\text{COO})$ interacting with the quinuclidine N. The “1:3, cyclic” spectrum looks very different compared to spectra of the other three 1:3 complexes. Particularly, the band at 1770 cm⁻¹, assigned to combination vibrations of $\nu_{\text{as}}(\text{COO})$ and $\delta(\text{O–H}[\cdots\text{N}])$ is prominent. For other 1:1, 1:2, and 1:3 complexes, this vibrational mode is located at a higher frequency than 1900 cm⁻¹, not depicted in Figure 6. This vibrational mode shifts remarkably depending on the characteristics of the hydrogen bond network. Nevertheless, such a band is expected to be fairly broad⁶¹ and likewise difficult to be observed under our experimental conditions. The spectrum calculated for the “1:3, halfN, cyclic”, the energetically

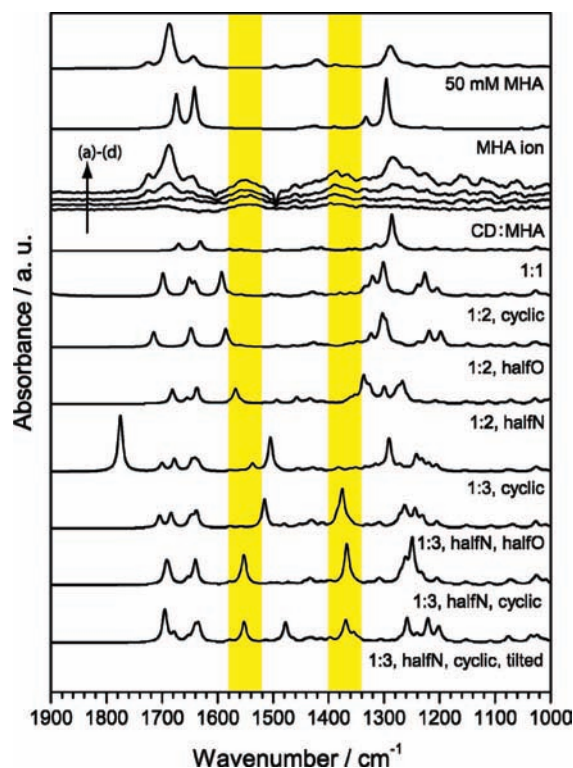


Figure 6. Comparison of the experimental MHA (Figure 3c) and CD + MHA (Figure 4a–d) IR spectra with the theoretical ones of the investigated CD–MHA complexes (Figure 5). The theoretical spectrum of the MHA anion is also shown as the reference of carboxylate vibrational frequencies without a biasing environment. The theoretical IR spectra were obtained by the B3PW91-G method, and the frequencies are scaled by 0.96.

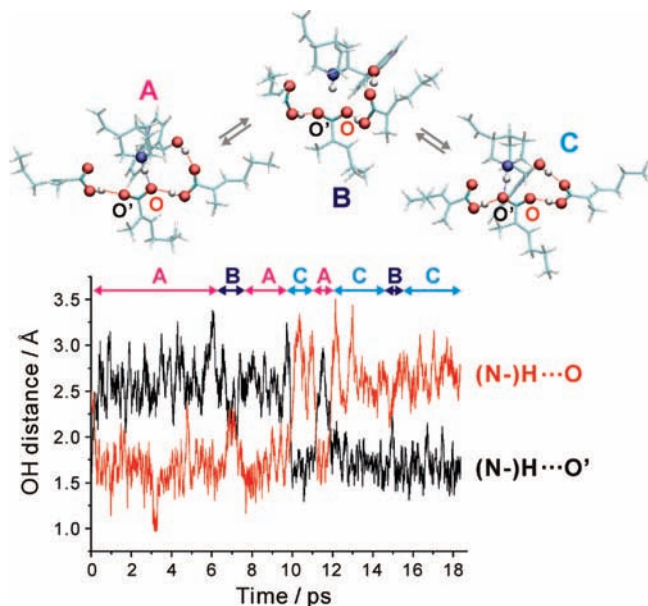


Figure 7. O–H bond length trajectories of MHA interacting with the quinuclidine N of CD during the ab initio molecular dynamics (18.4 ps). The initial complex structure was the “1:3, halfN, cyclic” complex (shown as C). The two different oxygen atoms in MHA are noted as O and O’.

most stable complex, reproduced best the spectral features arising from the CD–MHA interaction. The calculated spectrum for the “1:3, halfN, halfO” complex is close to the one of “1:3, halfN, cyclic”, however with slightly less agreement for $\nu_{\text{as}}(\text{COO})$ (Figure 6). Interestingly, the “1:3, halfN, cyclic, tilted” complex, only a little less stable than the “1:3, halfN, cyclic”, is expected to have an additional band at $\sim 1460 \text{ cm}^{-1}$, which may have appeared in the broad $\nu(\text{COO})$ bands. On the basis of the findings shown in Figure 6, we conclude that the interaction signals detected in the IR originate possibly from the “1:2, halfN”, the “1:3, halfN, halfO”, the “1:3, halfN, cyclic”, and the “1:3, halfN, cyclic, tilted” complexes, thus predominantly 1:3 complexes. In particular, the “1:3, halfN, cyclic” and the “1:3, halfN, cyclic, tilted” showed a very good agreement with the experimental IR spectra. Both DFT methods yielded the “1:3, halfN, cyclic” as the most stable complex, the “1:3, halfN, cyclic, tilted” coming second (Table 1), which confirms the reliability in the order of the complex stabilities. Interestingly, all four low-energy complexes have shorter H...N bonds, around 1.07 \AA , in contrast to the complexes whose spectra do not possess bands in the highlighted region. These specific forms of the hydrogen bond network can probably enhance the acidity of the MHA and the electrostatic interaction, leading to the larger stabilization.

Ab Initio Molecular Dynamics Study of the 1:3 Complex.

The stability of the “1:3, halfN, cyclic” complex and the conformational flexibility of the CD therein was examined by ab initio molecular dynamics using the BLYP-PW method. The purpose was to evaluate the flexibility and stability; therefore, the temperature of the system was controlled simply by velocity scaling at 300 K. Total simulation time extended over 18.4 ps. Figure 7 shows the trajectories of the O–H and O’–H distances, where O and O’ belong to the same MHA molecule which interacts with the quinuclidine N of CD. The initial configuration was C, “1:3, halfN, cyclic”. Upon the start of the simulation, instantaneously, the proton of the N–H...O’ hopped to O, resulting in the configuration A. This configuration A, not investigated previously, was stable for ~ 6.5 ps. Static DFT

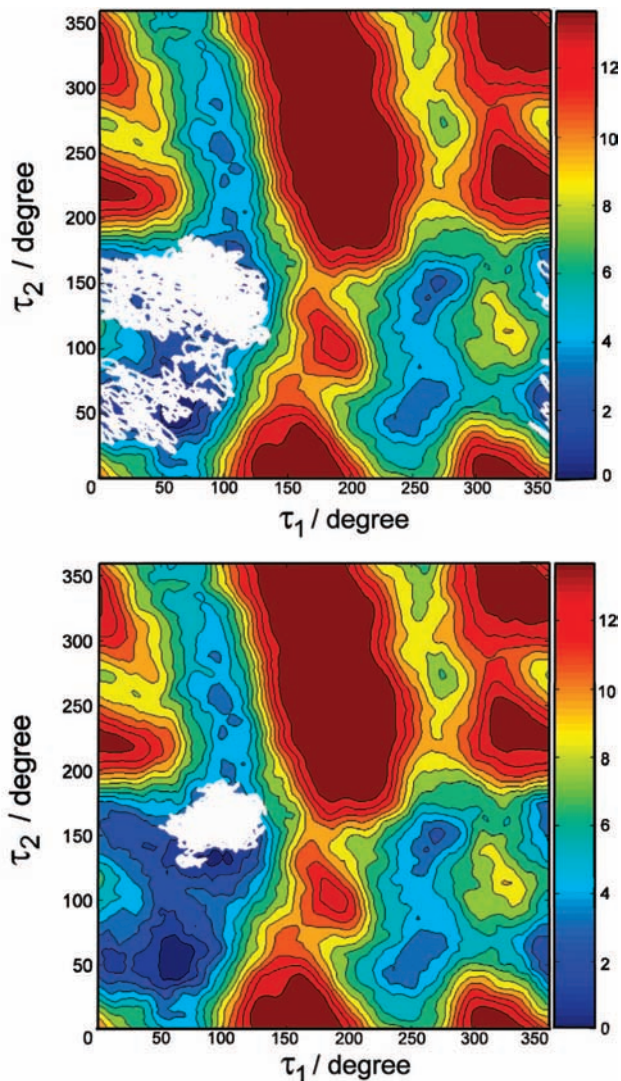


Figure 8. Conformational trajectory (τ_1 and τ_2) of CD during the ab initio molecular dynamics in its isolated form (upper panel) and within the “1:3, halfN, cyclic” complex (lower panel) at 300 K mapped on the free-energy surface of CD in vacuum at 300 K.⁵⁵ The simulation lengths were 23.9 and 18.4 ps, respectively. The energy bar on the right side is given in kcal mol^{-1} .

analysis showed configuration A to be less stable compared to all of the investigated 1:3 complexes before (Figure 5) and, in particular, destabilized by 2.6 kcal/mol relative to the configuration C based on the B3PW91-G method (zpe corrected). Still, configuration A seemed to be of similar stability as C at this temperature in vacuum. The configuration of the complex fluctuated between A, B, and C in the period of 6.5–12 ps. The configuration B has to be considered as a metastable state where two oxygen atoms are equivalently interacting with the N–H, forming a bifurcated bond. For times longer than 12 ps, the complex was stable mostly in the configuration C. Remarkably, the “1:3, halfN, cyclic” retained its configuration despite the switching to other stable configurations such as A and B. Since the conditions used in the simulation process give more freedom for molecular motion compared to that for the experiments due to the absence of solvent, we expect that the stability of the 1:3 complex could be further enhanced in solution, especially in apolar solvents. In polar solvents, the solvent molecules likely break the specific hydrogen bond network. This highly flexible and delocalized nature of the hydrogen bond network would lead to entropic stabilization, which might

TABLE 2: Interproton Distances and Dihedral Angles τ_1 , τ_2 , and τ_3 Obtained from the Optimized Structures by the Two DFT Methods and the Relative NOESY Cross Peak Volume of the Specific Proton Pairs

H-atom#	H-atom#	CD Open(3)	CD-3MHA, hN, cyc		relative NOESY cross peak volume	
		B3PW91-G	BLYP-PW	B3PW91-G	2.5 mM CD	2.5 mM CD, 5 mM MHA
5	8	2.149 Å	2.181 Å	2.176 Å	1.00	1.00
5	9	2.59 Å	2.551 Å	2.443 Å	0.45	0.63
8	16	2.679 Å	2.790 Å	2.703 Å	0.51	0.07
1	11	2.789 Å	2.644 Å	2.576 Å	0.14	0.25
	τ_1 /degree	98.7	101.5	102.7		
	τ_2 /degree	150.1	160.3	160.8		
	τ_3 /degree	278.2	288.7	288.8		

explain the superior stability of 1:3 complexes, particularly of the “1:3, halfN, cyclic” as seen from the best agreement between experimental and calculated IR spectra. The “1:3, halfN, cyclic tilted” can also be transformed from the “1:3, halfN, cyclic” via simple rotation of the central MHA molecule. The complex was indeed observed and included as a possible 1:3 interaction by a different run of *ab initio* molecular dynamics simulations at a slightly different temperature starting from the “1:3, halfN, cyclic”, suggesting that a likelihood of transitions between different types of stable 1:3 complexes exists. Judging from the similarity in stability of these complexes and the possible entropic enhancement of the hydrogen bond network of the “1:3, halfN, cyclic tilted” by short-range proton hopping to other oxygens of MHA and the possibility of formation of bifurcated bonds, the probability of finding both types of complexes is expected to be similar.

Furthermore, the conformational behavior of CD within the 1:3 complex was analyzed and compared with that of the isolated CD simulated under identical conditions except for the total simulation time (23.9 ps). Figure 8 shows the trajectories of the dihedral angles τ_1 and τ_2 during the two simulations, mapped in white onto the free-energy surface of the isolated CD at 300 K obtained by *ab initio* metadynamics.⁵⁵ At a first glance, we notice a clear difference of τ_1 and τ_2 trajectories between the CD in the 1:3 complex (Figure 8, lower panel) and the isolated CD (Figure 8 upper panel). The isolated CD was mostly in the Open(3) conformation (τ_1 : 99° and τ_2 : 150°, optimized by the BLYP-PW method), but it transformed into other conformations like Closed(2), Closed(7), and Open(8).⁵⁵ In contrast, the two torsional movements are largely restricted by the specific 1:3 interaction and centered at a slightly different minimum. The center of the trajectory was close to the values obtained for the “1:3, halfN, cyclic” (τ_1 : 102° and τ_2 : 160°, optimized by the BLYP-PW method). A slightly distorted Open(3) conformation within the 1:3 complex was also suggested by the detailed analysis of the NOESY spectra. In Table 2, interatomic distances between protons of less than 3 Å, characteristic of conformational discrimination of CD,⁵⁵ are listed. For the optimized Open(3) structure, the distance between H₈ and H₁₆ is smaller than that between H₁ and H₁₁; however, the former is larger in the CD within the “1:3, halfN, cyclic”. The same trend was confirmed by the order of the relative NOESY signal intensity that is also inverted for these proton pairs. This clearly points to the distorted Open(3) upon the interaction with MHA and the plausibility of the specific hydrogen bond network as discussed in this study. We found that the most stable 1:2 complex, the “1:2, halfN”, shows one of the characteristic $\nu(\text{COO})$ bands in the experimentally observed “CD–MHA interaction” region. However, this 1:2 complex is energetically less favorable than the 1:3 complexes and clearly less flexible than the probable 1:3 complexes due to the bidentate interaction of MHA with CD (Figure 5),

although the 1:2 cinchona–carboxylic acid ratio has been accepted as the intermediate modifier–acid complex for the hydrogenation of aliphatic acids.^{5,33,56}

It is noteworthy that the interaction scheme can be extended to include even more acid molecules with respect to the modifier, for example, 1:4 and 1:5 complexes. Due to the expected very flexible hydrogen bond networks of such complexes, a more sophisticated approach such as QM/MM might be needed, including explicit solvent molecules with molecular dynamics to study the statistical behavior of such complexes and the network. Still, we strongly believe that the 1:3 structural motives reported here constitute the backbone moieties of the extended hydrogen bond network since there is little space left for additional hydrogen bonds within the central core. The results of this study, the form of the specific hydrogen bond network, may clarify some aspects of the hydrogenation on surface. The state of CD–MHA complex in the presence of the Pd surface is currently under investigation.

Conclusions

The combined NMR, IR, and theoretical study suggested a new mode of interaction between the chiral modifier, CD, and the carboxylic acid, MHA. The population of the 1:1 CD–MHA complex seems minor, while that of the 1:2 complex may exist in a small portion. Instead, the 1:3 complex likely exists abundantly in toluene solution. Especially, “1:3, halfN, cyclic” and also the “1:3, halfN, cyclic tilted” types of complexes are found to be stable due to a specific yet flexible set of hydrogen bond networks. The stability of the complexes was assessed by two different DFT methods and also *ab initio* molecular dynamics, helping to explain the experimental spectral changes observed in IR and NMR. This study can be considered as a reference with regard to the surface structure of the complexes, where a chiral surface site is formed during the asymmetric hydrogenation.

Acknowledgment. The Swiss National Science Foundation is acknowledged for financial support. We thank Dr. Ronny Wirz, Dr. Davide Ferri, and Dr. Tamas Mallat for experimental support and helpful discussions.

Supporting Information Available: ¹H, HH-COSY, and HH-TOCSY spectra of CD. ¹H and HH-NOESY spectra of CD + MHA. This material is available free of charge via the Internet at <http://pubs.acs.org>.

References and Notes

- Lehn, J. M. *Angew. Chem., Int. Ed. Engl.* **1990**, *29*, 1304.
- Mo, J.; Xiao, J. L. *Angew. Chem., Int. Ed.* **2006**, *45*, 4152.
- Lee, J. M.; Ahn, D. S.; Jung, D. Y.; Lee, J.; Do, Y.; Kim, S. K.; Chang, S. K. *J. Am. Chem. Soc.* **2006**, *128*, 12954.

- (4) Martinek, T. A.; Varga, T.; Fülöp, F.; Bartók, M. *J. Catal.* **2007**, *246*, 266.
- (5) Borszékly, K.; Mallat, T.; Baiker, A. *Catal. Lett.* **1996**, *41*, 199.
- (6) Blaser, H. U.; Jalett, H. P.; Muller, M.; Studer, M. *Catal. Today* **1997**, *37*, 441.
- (7) Sípós, E.; Tungler, A.; Fogassy, G. *J. Mol. Catal. A: Chem.* **2004**, *216*, 171.
- (8) Studer, M.; Blaser, H. U.; Exner, C. *Adv. Synth. Catal.* **2003**, *345*, 45.
- (9) Kacprzak, K.; Gawronski, J. *Synthesis* **2001**, 961.
- (10) Baiker, A. *Catal. Today* **2005**, *100*, 159.
- (11) Mallat, T.; Orglmeister, E.; Baiker, A. *Chem. Rev.* **2007**, *107*, 4863.
- (12) Mallat, T.; Diezi, S.; Baiker, A. *Handbook of Heterogeneous Catalysis*, 2nd ed.; Ertl, G., Knözinger, H., Schüth, F., Weitkamp, J., Eds.; VCH: Weinheim, Germany, 2008; Vol. 7, pp 3603–3626.
- (13) Nitta, Y.; Watanabe, J.; Okuyama, T.; Sugimura, T. *J. Catal.* **2005**, *236*, 164.
- (14) Szöllösi, G.; Balázsik, K.; Bartók, M. *Appl. Catal. A* **2007**, *319*, 193.
- (15) Sugimura, T.; Watanabe, J.; Uchida, T.; Nitta, Y.; Okuyama, T. *Catal. Lett.* **2006**, *112*, 27.
- (16) Szöllösi, G.; Hanaoka, T.; Niwa, S.; Mizukami, F.; Bartók, M. *J. Catal.* **2005**, *231*, 480.
- (17) Takaya, H.; Ohta, T.; Noyori, R. *Asymmetric Hydrogenation*; VCH Publishers, Inc.: New York, 1993.
- (18) Chapuis, C.; Jacoby, D. *Appl. Catal. A* **2001**, *221*, 93.
- (19) Szöllösi, G.; Niwa, S. I.; Hanaoka, T. A.; Mizukami, F. *J. Mol. Catal. A: Chem.* **2005**, *230*, 91.
- (20) Hermán, B.; Szöllösi, G.; Fülöp, F.; Bartók, M. *Appl. Catal. A* **2007**, *331*, 39.
- (21) Berg, U.; Aune, M.; Matsson, O. *Tetrahedron Lett.* **1995**, *36*, 2137.
- (22) Bürgi, T.; Baiker, A. *J. Am. Chem. Soc.* **1998**, *120*, 12920.
- (23) Dijkstra, G. D. H.; Kellogg, R. M.; Wynberg, H. *J. Org. Chem.* **1990**, *55*, 6121.
- (24) Dijkstra, G. D. H.; Kellogg, R. M.; Wynberg, H. *Recl. Trav. Chim. Pays-Bas* **1989**, *108*, 195.
- (25) Sai, T.; Takao, N.; Sugiura, M. *Magn. Reson. Chem.* **1992**, *30*, 1041.
- (26) Szöllösi, G.; Chatterjee, A.; Forgó, N.; Bartók, M.; Mizukami, F. *J. Phys. Chem. A* **2005**, *109*, 860.
- (27) Dijkstra, G. D. H.; Kellogg, R. M.; Wynberg, H.; Svendsen, J. S.; Marko, I.; Sharpless, K. B. *J. Am. Chem. Soc.* **1989**, *111*, 8069.
- (28) Schürch, M.; Schwalm, O.; Mallat, T.; Weber, J.; Baiker, A. *J. Catal.* **1997**, *169*, 275.
- (29) Vargas, A.; Bonalumi, N.; Ferri, D.; Baiker, A. *J. Phys. Chem. A* **2006**, *110*, 1118.
- (30) Ferri, D.; Bürgi, T.; Baiker, A. *J. Chem. Soc., Perkin Trans. 2* **1999**, 1305.
- (31) Olsen, R. A.; Borchardt, D.; Mink, L.; Agarwal, A.; Mueller, L. J.; Zaera, F. *J. Am. Chem. Soc.* **2006**, *128*, 15594.
- (32) Ferri, D.; Bürgi, T.; Borszékly, K.; Mallat, T.; Baiker, A. *J. Catal.* **2000**, *193*, 139.
- (33) Ferri, D.; Bürgi, T.; Baiker, A. *J. Chem. Soc., Perkin Trans. 2* **2002**, 437.
- (34) Hall, T. J.; Johnston, W. A. H.; Vermeer, S. R.; Watson, P. B. *Stud. Surf. Sci. Catal.* **1996**, *101*, 221.
- (35) Nitta, Y.; Shibata, A. *Chem. Lett.* **1998**, 161.
- (36) Bisignani, R.; Franceschini, S.; Piccolo, O.; Vaccari, A. *J. Mol. Catal. A: Chem.* **2005**, *232*, 161.
- (37) Borszékly, K.; Bürgi, T.; Zhaohui, Z.; Mallat, T.; Baiker, A. *J. Catal.* **1999**, *187*, 160.
- (38) Borszékly, K.; Mallat, T.; Baiker, A. *Tetrahedron: Asymmetry* **1997**, *8*, 3745.
- (39) Nitta, Y.; Kubota, T.; Okamoto, Y. *J. Mol. Catal. A: Chem.* **2004**, *212*, 155.
- (40) Razkin, J.; Gil, P.; Gonzalez, A. *J. Chem. Ecol.* **1996**, *22*, 673.
- (41) Uccellobarretta, G.; Dibari, L.; Salvadori, P. *Magn. Reson. Chem.* **1992**, *30*, 1054.
- (42) Ma, Z.; Zaera, F. *J. Phys. Chem. B* **2005**, *109*, 406.
- (43) Urakawa, A.; Wirz, R.; Bürgi, T.; Baiker, A. *J. Phys. Chem. B* **2003**, *107*, 13061.
- (44) Bürgi, T.; Baiker, A. *Adv. Catal.* **2006**, 227.
- (45) Baurecht, D.; Fringeli, U. P. *Rev. Sci. Instrum.* **2001**, *72*, 3782.
- (46) Urakawa, A.; Bürgi, T.; Baiker, A. *Chem. Eng. Sci.* In Press.
- (47) Perdew, J. P.; Wang, Y. *Phys. Rev. B* **1992**, *45*, 13244.
- (48) Becke, A. D. *Phys. Rev. A* **1988**, *38*, 3098.
- (49) Frisch, M. J.; Trucks, G. W.; Schlegel, H. B.; Scuseria, G. E.; Robb, M. A.; Cheeseman, J. R.; Montgomery, J. A., Jr.; Vreven, T.; Kudin, K. N.; Burant, J. C.; Millam, J. M.; Iyengar, S. S.; Tomasi, J.; Barone, V.; Mennucci, B.; Cossi, M.; Scalmani, G.; Rega, N.; Petersson, G. A.; Nakatsuji, H.; Hada, M.; Ehara, M.; Toyota, K.; Fukuda, R.; Hasegawa, J.; Ishida, M.; Nakajima, T.; Honda, Y.; Kitao, O.; Nakai, H.; Klene, M.; Li, X.; Knox, J. E.; Hratchian, H. P.; Cross, J. B.; Bakken, V.; Adamo, C.; Jaramillo, J.; Gomperts, R.; Stratmann, R. E.; Yazyev, O.; Austin, A. J.; Clifford, S.; Cioslowski, J.; Stefanov, B. B.; Liu, G.; Liashenko, A.; Piskorz, P.; Komaromi, I.; Martin, R. L.; Fox, D. J.; Keith, T.; Al-Laham, M. A.; Peng, C. Y.; Nanayakkara, A.; Challacombe, M.; Gill, P. M. W.; Johnson, B.; Chen, W.; Wong, M. W.; Gonzalez, C.; Pople, J. A. *Gaussian 03*, revision C.02; Gaussian, Inc.: Pittsburgh, PA, 2004.
- (50) Lee, C. T.; Yang, W. T.; Parr, R. G. *Phys. Rev. B* **1988**, *37*, 785.
- (51) www.cpmid.org. IBM Corp, MPI für Festkoerperforschung: Stuttgart, Germany, 1997–2001.
- (52) Boys, S. F.; Bernardi, F. *Mol. Phys.* **1970**, *19*, 553.
- (53) Troullier, N.; Martins, J. L. *Phys. Rev. B* **1991**, *43*, 8861.
- (54) Bürgi, T.; Vargas, A.; Baiker, A. *J. Chem. Soc., Perkin Trans. 2* **2002**, 1596.
- (55) Urakawa, A.; Meier, D. M.; Rüegger, H.; Baiker, A. *J. Phys. Chem. A* **2008**, in press.
- (56) Kun, I.; Török, B.; Felföldi, K.; Bartók, M. *Appl. Catal. A* **2000**, *203*, 71.
- (57) Ferri, D.; Bürgi, T.; Baiker, A. *Phys. Chem. Chem. Phys.* **2002**, *4*, 2667.
- (58) Pretsch, E.; Bühlmann, P.; Affolter, C.; Badertscher, M. *Spektroskopische Daten zur Strukturaufklärung organischer Verbindungen*; Springer: Berlin, Germany, 2001.
- (59) Schwalm, O.; Weber, J.; Margitfalvi, J.; Baiker, A. *J. Mol. Struct.* **1993**, *297*, 285.
- (60) Carneiro, J. W. D.; de Oliveira, C. D.; Passos, F. B.; Aranda, D. A. G.; Rogerio, P.; de Souza, P. R. N.; Antunes, O. A. C. *Catal. Today* **2005**, *107–108*, 31.
- (61) Bonalumi, N.; Bürgi, T.; Baiker, A. *J. Am. Chem. Soc.* **2003**, *125*, 13342.